Eur. Phys. J. A **6**, 197–202 (1999)

THE EUROPEAN PHYSICAL JOURNAL A

Thermal and chemical equilibrium for vaporizing sources*

The INDRA Collaboration

B. Borderie[1], F. Gulminelli[2], M.F. Rivet[1], L. Tassan-Got[1], M. Assenard[3], G. Auger[4], F. Bocage[2], R. Bougault[2], R. Brou[2], Ph. Buchet[5], J. Colin[2], R. Dayras[5], A. Demeyer[6], J.D. Frankland[1], E. Galichet[6], E. Genouin-Duhamel[2], E. Gerlic[6], M. Germain[3], D. Guinet[6], P. Lautesse[6], J.L. Laville[3], J.F. Lecolley[2], T. Lefort[2], R. Legrain[5], N. Le Neindre[2], M. Louvel[2], A.M. Maskay[6], L. Nalpas[5], A.D. Nguyen[2], M. Parlog[7], E. Plagnol[1], A. Rahmani[3], T. Reposeur[3], E. Rosato[8], F. Saint-Laurent[4a], S. Salou[4], J.C. Steckmeyer[2], M. Stern[6], G. Tabacaru[7], B. Tamain[2], O. Tirel[4], D. Vintache[2], C. Volant[5]

[1] Institut de Physique Nucléaire, IN2P3-CNRS, 91406 Orsay cedex, France
[2] LPC, IN2P3-CNRS, ISMRA et Université, 14050 Caen cedex, France
[3] SUBATECH, Ecole des Mines, IN2P3-CNRS et Université, 44072 Nantes cedex 03, France
[4] GANIL (DSM-CEA/IN2P3-CNRS), B.P.5027, 14021 Caen cedex, France
[5] DAPNIA/SPhN, CEA/Saclay, 91191 Gif sur Yvette cedex, France
[6] Institut de Physique Nucléaire, IN2P3-CNRS et Université, 69622 Villeurbanne cedex, France
[7] National Institute for Physics and Nuclear Engineering, 76900 Bucharest-Magurele, Romania
[8] Dipartimento di Scienze Fisiche e Sezione INFN, Univ. di Napoli "Federico II", 80126 Napoli,Italy

Received: 6 April 1999
Communicated by P. Schuck

Abstract. Vaporized sources produced in collisions between ^{36}Ar and ^{58}Ni at 95 MeV per nucleon have been detected with the multidetector INDRA. Complete information concerning the deexcitation properties of quasi-projectiles, including second moments of chemical composition, is compared to a quantum statistical model describing a gas of fermions and bosons in thermal and chemical equilibrium. Inclusions in the calculation of all known discrete levels of nuclear species which deexcite into light particles and of a final state excluded volume interaction are found decisive to very well reproduce the experimental data, which strongly supports that thermodynamical equilibrium was achieved at freeze-out for such sources.

PACS. 25.70.-z Low and intermediate energy heavy-ion collisions – 24.60.-k Statistical theory and fluctuations – 25.70.Pq Multifragment emission and correlations

1 Introduction

At present there exist many models, describing a simultaneous disassembly of highly excited nuclear sources produced in nucleus-nucleus collisions at intermediate energies, which presuppose that before disintegrating these sources achieve partial or complete thermodynamical equilibrium [1–6]. This hypothesis is essential if one wants to describe the sources by means of macroscopic variables such as pressure and density at finite temperature. However such an assumption is *a priori* not obvious if we bear in mind the shortening of all time scales with respect to those involved at low and moderate excitation energies. The very fundamental question of the degree of equilibrium reached can be only answered by confronting statistical models to complete data on the deexcitation of well identified nuclear sources provided by highly efficient multidetector systems.

Here we report on a detailed comparison of the properties of vaporized quasi-projectiles (QP) produced in binary dissipative collisions between ^{36}Ar and ^{58}Ni nuclei at 95 AMeV incident energy with a quantum statistical model. Particularly, the completeness of the selected sources made possible the extraction of variances for multiplicities of the different emitted charged particles, thus permitting a more stringent comparison with the model. Apart from the completeness of information, these sources are also interesting because they represent an extreme deexcitation mode for hot pieces of nuclear matter, close to the intuitive expectation of a supercritical nuclear gas [7,8].

2 Experimental procedure

The experiment was performed using a 95 AMeV ^{36}Ar beam with an intensity of 3-4 10^7 pps delivered by the

* *Experiment performed at Ganil*
[a] *present address: DRFC/STEP, CEA/Cadarache, F-13108 Saint Paul lez Durance Cedex, France*

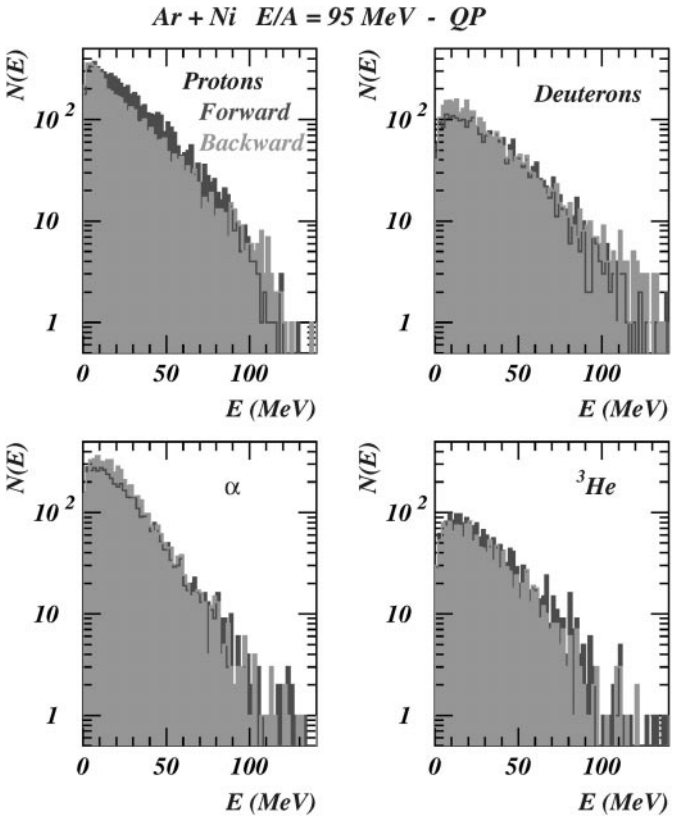

Fig. 1. Energy spectra of particles emitted by the QP in forward and backward direction with respect to the QP velocity

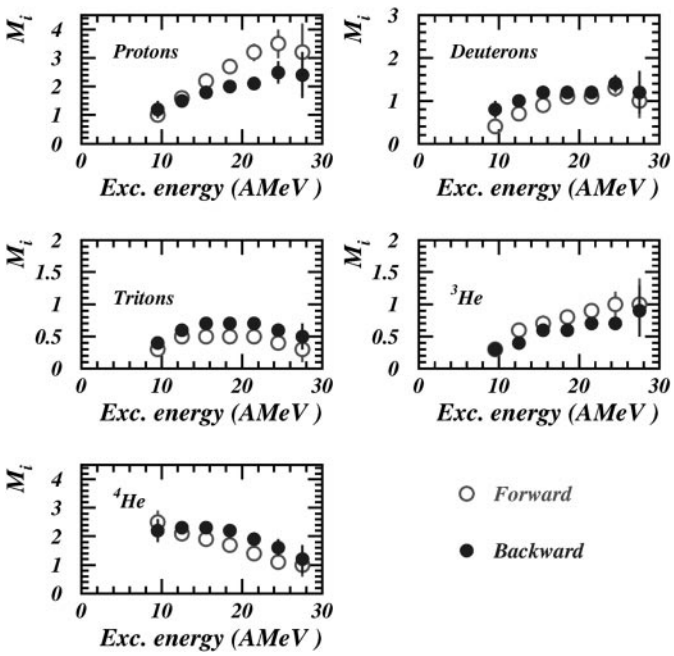

Fig. 2. Forward and backward multiplicities of particles emitted by the QP in its frame as a function of its excitation energy obtained from calorimetry

GANIL facility. Experimental details have already been reported in [9–11]. Briefly, charged products were detected by the INDRA detector [12] with a geometric acceptance of 90% of 4π and isotopic separation was achieved up to Z=3. Absolute energy calibrations are estimated to be accurate to within 5%. Concerning the identification thresholds, for hydrogen isotopes the separations between protons-deuterons and deuterons-tritons are obtained for energies greater than 6 MeV and 8 MeV respectively and the separation for helium isotopes is achieved above 25 MeV. As a consequence of these thresholds in the laboratory frame only particles emitted from QP are detected without any bias.

The sample here analyzed is exactly the same as in [10, 11]. Vaporization events, where all produced species have atomic number lower than 3, have been selected by imposing that more than 90% of the charge of the system was detected. Neutrons, which represent 15% of the total mass of the system, are not detected but their multiplicities are derived from mass conservation; their energies were estimated from those of protons, and neutron multiplicities of QP were built assuming the N/Z ratio of the system. Vaporization events were produced over an estimated impact parameter range 0-3.5 fm. A two source reconstruction (quasi-projectile and quasi-target) using the thrust analysis [13] was performed to determine the source velocities. Recently many studies of mid-rapidity or neck emissions [14–16] have appeared. We found then important to strengthen, for the vaporization events, the proposed binary scenario [10] by giving strong additional information in support of such an analysis. We present in figures 1 and 2 a comparison between the forward and backward energy spectra and multiplicities (at different excitation energies) of the different particles emitted by the reconstructed vaporized QP. Only small and non-systematic forward-backward variations are seen, which argues for emission by an equilibrated QP in a rather pure binary scenario. Deviations on multiplicities, for example, do not show any increase with excitation energy (i.e. centrality) as it would be expected for a contamination from mid-rapidity or neck emissions. The only visible preequilibrium effect is a slight enhancement of forward proton emission. Another strong argument against an important contamination from dynamical emissions is that the observables discussed in this paper are independent of the beam energy (from 52 to 95 AMeV) and depend only on the excitation energy of the source. The only variable depending on the beam energy is the vaporization cross section [9]. On the other hand it is claimed in [15] that a clear signature of mid-rapidity emission was an increase of transverse energy for particles emitted in this rapidity region. We do observe such an increase but reduced as compared to non-vaporized events. Keeping in mind that vaporization events are far from representing the most probable exit channel of the reaction, we intuitively expect mid-rapidity or neck emissions to be minimized in our specific event sample: the maximum energy should be deposited in the reaction partners in order to vaporize both of them. Moreover at the high excitation energies implied in vaporization the different time scales for emission are very short and become comparable. Therefore it may not be meaningful to separate the emission mechanism into a fast component (preequi-

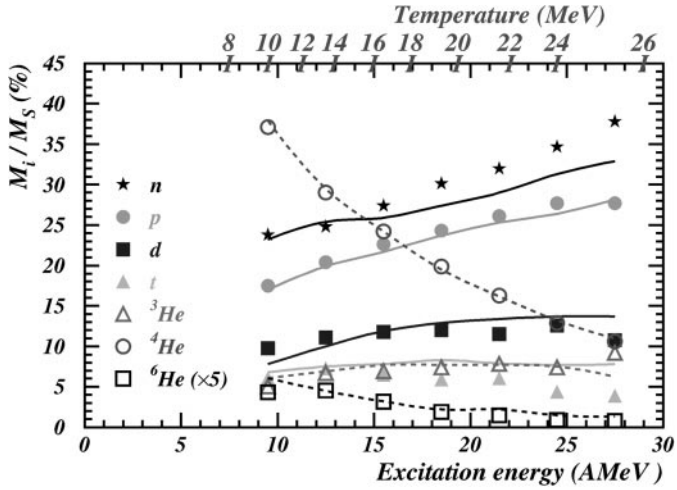

Fig. 3. Composition of the QP as a function of its excitation energy. Symbols are for data while the lines (dashed for He isotopes) are the results of the model. The temperature values used in the model are also given (see text)

librium particles emitted at mid-rapidity and at forward and backward angles) and a slow one (emission from equilibrated sources): a detailed study of mid-rapidity emission performed on the same system, but for all events, clearly shows that the chemical compositions of particles emitted at mid-rapidity or by the QP become similar when excitation energies larger than 10 AMeV are involved [17]. Considering all the previous arguments it is reasonable for the comparison discussed hereafter to work in the frame of a pure binary scenario.

Deexcitation properties and characteristics of QP have already been reported in ref [11] using an excitation energy per nucleon binning of 3 AMeV: reconstructed QP masses increase from 31 to 37 when excitation energy varies from 8 to 15 AMeV, and then stay constant around 37-38 at higher excitation energy while QP multiplicities increase monotonously from 13 to 22 over the whole energy range.

The emission properties displayed in Figs. 1 and 2 are a necessary but not sufficient condition for thermal equilibrium. In the following we shall determine to which extent deexcitation properties of vaporized sources can be described, in detail, by a model of quantal gas in thermodynamical equilibrium [18] including a simplified final state interaction and side feeding.

3 Thermodynamical equilibrium model

In the model the emitting source is supposed to undergo a simultaneous disassembly at fixed temperature T, density ρ and isospin (N/Z) into a gas of fermions and bosons in thermal and also chemical equilibrium [19]. Calculations are performed within the grand canonical ensemble. This ensemble is generally used for infinite systems but such an approximation for finite systems is justified at very high excitation energies when the multiplicity of particles is large: typically larger than 5 for the involved QP masses [2]. Thus at a given density and temperature the relative yields and the energy spectra of the different nuclear species emitted by the source are uniquely determined from conservation laws and the equilibrium distributions in the grand canonical ensemble. To compare to the selected data sample the conditional probability of the partition under the constraint of vaporization has to be evaluated. This is achieved by including in the partition sum all known discrete levels of nuclear species up to ^{20}Ne [20] which after deexcitation give only n, H, and He isotopes. With this procedure the relative contribution of the different particle species can be compared to data without any bias, but of course no information about the cross-section of the vaporization channel can be extracted. In this formalism the discrete levels of the different isotopes are treated as independent structureless particles characterized by an internal energy augmented with respect to the ground state binding energy, and by their proper degeneracy factor. This corresponds to the implicit assumption that these states are sufficiently narrow, i.e. their life time is much longer than the equilibration time. Thus in the calculation only levels with widths equal to or lower than a cutoff value Γ_0 are included in the state sum. In the following, Γ_0= 2 MeV will be employed which corresponds to state life-times larger than about 100 fm/c. Corrections to an ideal gas are included in the form of excluded volume effects in the spirit of the Van der Waals gas to deal with collisions and reabsorption at freeze-out [18]. The consequence of the excluded volume approximation employed by [18] is to favour protons, neutrons and alphas over the more loosely bound structures like deuterons and high-lying resonances. Finally the calculated distributions are corrected for the side-feeding from resonance decays. Since the probability of a partition is factorized into the emission probabilities of fragments, events can be easily generated by successively drawing particles and their kinetic energy according to the conditional grand canonical partition function up to a source mass

$$A_s^k = \sum_{i=1}^{m_k} A_i \tag{1}$$

and a source excitation energy

$$\varepsilon_s^k . A_s^k = \sum_{i=1}^{m_k} (E_i + B_i + V_i) - B_s \tag{2}$$

Here m_k is the multiplicity of event k and A_i, E_i, B_i are the mass, kinetic energy and binding energy of the $i-$th particle of the event; V_i is the average inter-particle Coulomb energy assumed independent of the freeze-out configuration and approximated by

$$\frac{3}{5}\frac{Z_i(< Z_s > - Z_i)e^2}{< R_s >} \tag{3}$$

The subscript s refers to the source and the averages are taken over events corresponding, for the comparison to the data, to a 3 AMeV binning for ε_s. For given temperature, density and chemical potentials the first moments of

the particle multiplicity distributions are univocally given by the general laws of statistical mechanics. In a previous paper [11] the analytically calculated average multiplicities were compared to the same set of data; the temperature and chemical potentials were fixed from the experimental average excitation energy and mass, and density was a free parameter.

A Metropolis event generator is here introduced to extend the comparison of [11] to the second moment σ_i^2 of the multiplicity distributions of the different species. In principle one may argue that even the second moments can be calculated analytically: σ_i^2 depends on both the variances and mean values of the source parameters A_s and ε_s, the fluctuations of the source parameters in the grand canonical ensemble arising from the random exchanges of particles and energy with the thermal bath. However experimentally it is observed that no thermal equilibrium is achieved between the two partners of the reaction, due to short reaction times [10,21]. This means that the quasi target (QT) cannot be considered as a thermal bath for the QP, and that the observed fluctuations in mass and excitation energy of the sources are not directly connected to chemical potentials and temperature but are also due to fluctuations in the dynamics of the entrance channel and to the data selection requirements. Therefore the variances of the multiplicities of the emitted particles will have, together with a thermal component, a contribution coming from mass and energy fluctuations during the formation of the sources. To include this component, the mass and excitation energy distributions of the sources have been taken from experimental data as an input to the calculation. This prescription does not modify the first moments of multiplicities but is expected to have an effect on higher order moments.

To cover the experimental ε^* range the temperature had to be varied from 10 to 25 MeV. Isospin (N/Z) was fixed to 1, which is very close to the N/Z of the system. Finally the freeze-out density has been fixed to $\rho = \rho_0/3$, in order to reproduce the experimental ratio between the proton and alpha yields at ε^*=18.5 MeV.

4 Comparison to the model

The results of the model correspond to lines in Fig. 3 and to full lines in Fig. 4 and in Fig. 5.

4.1 Chemical composition (first moments)

Chemical compositions (first moments) as a function of the excitation energy are very well reproduced. Figure 3 exhibits the evolution of the relative particle abundance M_i/M_s where M_s is the total source multiplicity. Two elements were found essential to get such an agreement. First, the excluded volume correction which was already used in [11]: in the ideal gas case, the experimental proton over deuteron ratio would be fitted only by imposing a freeze-out density so low that the proton over alpha ratio would be overestimated by more than one order of magnitude

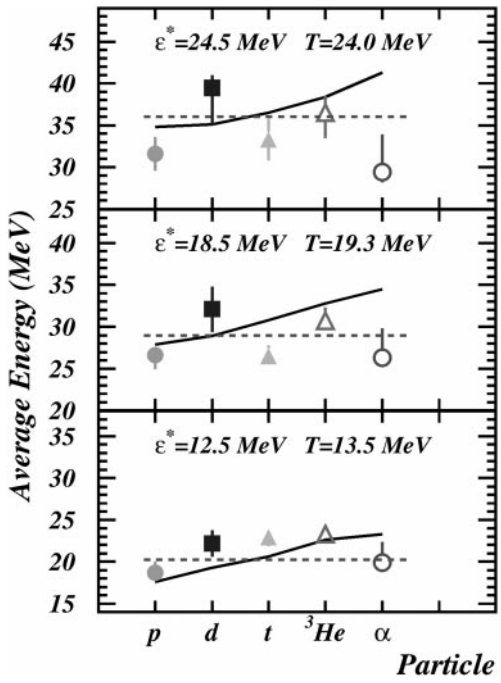

Fig. 4. Average kinetic energies of particles emitted by the QP at different excitation energies per nucleon. Symbols are for data while the full lines are the results of the model.The dashed lines refer to average kinetic energies of particles expected for an ideal gas ($\frac{3}{2}$T) at temperatures derived from the model. For error bars see text

[18]. And second, the extension of the mass table which has been used here (only species up to ^9B were included in the partition sum of [11]). As compared to [11], neutron, triton and ^3He relative abundances are better reproduced. The calculated primary multiplicities increase from 10 to 18 over the excitation energy range, which indicates that secondary decays are responsible for around 20% of final multiplicities. Secondary decays contribute especially to the alpha, proton and neutron yields with major contributions from three unstable nuclei: ^5He, $^6He^*$ and ^6Be; in particular secondary alpha emission represents more than 50% of the alpha yield.

4.2 Average kinetic energies

The average kinetic energies of the different particles are also rather well reproduced over the whole excitation energy range (see Fig. 4). But the model fails to accurately follow the dependence on the different species especially at high excitation energy. More generally the average kinetic energies are not very sensitive to reasonable variations of the different parameters. The energy differences between particles in the model are essentially due to Coulomb effects and to side-feeding. The slight but systematic overestimation of the alpha kinetic energies observed could indicate that the yield from resonances is relatively low since secondary decays tend to increase the average energy of alpha particles. However the influence on the yields and

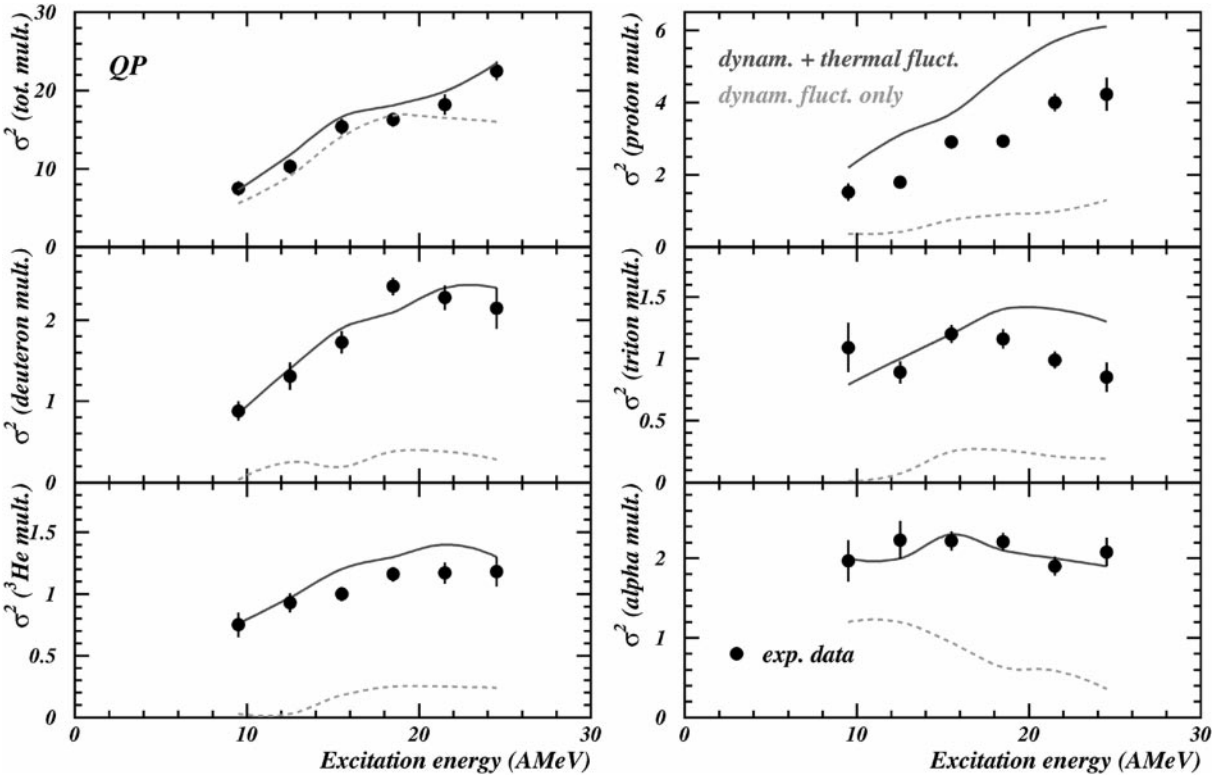

Fig. 5. Variances of multiplicity distributions (total, proton, deuton, triton, ^3He and alpha) of the QP as a function of its excitation energy per nucleon. Points refer to the data and the lines are the results of the model (see text). Error bars are statistical errors

average kinetic energies of the cut-off width of resonances, when varied in the range 0.5-5.0 MeV, is only a few percent. The dashed lines in Fig. 4 indicate the average kinetic energies, $\frac{3}{2}$T, expected for an ideal gas. These values are found to be a rather good approximation, which is due to the low density of the emitting sources. Experimental error bars in the figure give the limits obtained when different methods for reconstructing the sources are applied (thrust analysis considering all the particles or only particles with A>2). The last parameter to be discussed is the freeze-out density, which is the only critical parameter of the model, and was fixed to reproduce the experimental relative yield between protons and alphas. A change in the density only very slightly affects the kinetic energies, but produces a sizeable modification in the production yields. Protons and deuterons are increasingly favoured over alphas as the density decreases [22].

4.3 Chemical composition (second moments)

To further test the predictions of the model we have compared the second moments of the distributions, namely the variances of the particle multiplicities. Both in data and calculations the variances are determined for excitation energy bins of 3 AMeV and we have checked that the values are independent of the binning (within the range 1-3 AMeV). The comparison data-calculations is displayed in Fig. 5 for the variances associated with the total multiplicity and with the different charged particle multiplicities. The order of magnitude is correctly reproduced by the calculation (full lines), as well as the evolution with the excitation energy. Note that variances for protons are systematically overestimated; an explanation for that can be possibly found in the presence, experimentally observed (see Fig. 1 and 2), of a non-equilibrium proton emission at forward angles. The dominance of the thermal origin to produce the observed fluctuations is demonstrated by a simulation where, at each excitation energy, the relative multiplicities and kinetic energies of the different particle species (in each event) are fixed to the average values for the corresponding excitation energy bin; only the total mass A_s of the event is allowed to vary with a width fixed by the experimental distribution. In this way only the fluctuations coming from the event selection criteria and from the dynamics of the entrance channel of the reaction are taken into account and thermal fluctuations are frozen. Variances on the total multiplicity are well reproduced by this calculation while the fluctuations observed for the different particles (dashed curves) are very small compared to experimental values. This means that the total multiplicity distribution is trivially related to the mass width of the vaporizing source; this source size effect obviously produces some width for the multiplicity distributions of the different emitted species as well, but these positively correlated widths are insufficient to explain the observed

variances which are found to be dominated by the uncorrelated thermal component. The correct prediction of the measured variances, besides that of the other observables, reinforces the idea that thermodynamical equilibrium has been reached.

5 Conclusions

The yields (mean values and variances) and the average kinetic energy of the different species emitted by vaporizing sources in collisions between ^{36}Ar and ^{58}Ni have been compared with the predictions of a model describing the properties of a quantum weakly-interacting gas of nuclear species in thermal and chemical equilibrium. Experimental observables are rather well reproduced, which gives strong confidence in the fact that thermodynamical equilibrium has been reached even for these sources produced in very extreme conditions and consequently that thermodynamics can be applied for such small systems. The scenario producing such sources may be the following: after an interaction time of around 40 fm/c (estimated from the time needed by the two nuclei to pass through each other), partners of collisions are on the way to thermalization. Then, due to the very high excitation energies involved, the partners start to dissociate and reach a density around $\rho = \rho_0/3$ within about 30fm/c (see for example [23,24]). Finally at low density and at very high temperatures in the supercritical region of the phase diagram [7,8], the emission properties of vaporized sources at freeze-out are fixed by thermodynamical equilibrium.

References

1. J. Randrup and S.E. Koonin, Nucl. Phys. **A356** (1981) 223
2. J. Bondorf et al., Phys. Rep. **257** (1995) 133 and references therein
3. D.H.E. Gross, Rep. Prog. Phys. **53** (1990) 605 and references therein
4. J. A. Lopez and J. Randrup Nucl. Phys. **A503** (1989) 183, Nucl. Phys. **A512** (1990) 345
5. H. Stöcker and W. Greiner, Phys. Rep. **5** (1986) 277; J. Konopka et al., Phy. Rev. **C50** (1994) 2085
6. W. A. Friedman, Phys. Rev. Lett. **60** (1988) 2125, Phys. Rev. **C42** (1990) 667
7. H. R. Jaqaman et al., Phys. Rev. **C29** (1984) 2067
8. J. N. De et al., Phys. Rev. **C55** (1997) R1641
9. C.O. Bacri et al., Phys. Lett. **B353** (1995) 27
10. M.F. Rivet et al., Phys. Lett. **B388** (1996) 219
11. B. Borderie et al., Phys. Lett. **B388** (1996) 224
12. J. Pouthas et al., Nucl. Instr. Meth. in Phys. Res. **A357** (1995) 418, **A369** (1996) 222
13. J. Cugnon and D. L'Hote, Nucl. Phys. **A397** (1983) 519
14. J. Péter et al., Nucl. Phys. **A593** (1995) 95
15. J. C. Angélique et al., Nucl. Phys. **A614** (1997) 261
16. Y. Larochelle et al., Phys. Rev. **C55** (1997) 1869, Phys. Rev. **C57** (1998) R1027
17. T. Lefort et al., submitted to Nucl. Phys. A
18. F. Gulminelli and D. Durand, Nucl. Phys. **A615** (1997) 117
19. A. Z. Mekjian, Phys. Rev. **C17** (1978) 1051; S. Das Gupta and A. Z. Mekjian, Phys. Rep. **72** (1981) 131
20. J. Konopka, private communication; F. Ajzenberg-Selove, Nucl. Phys. **A320,449,475,506,521,564** (1979-1993)
21. B. Borderie et al., Z. Phys. **A 357** (1997) 7 and references therein
22. F. Gulminelli et al., Proc. of the Int. Winter Meeting on Nuclear Physics, Bormio, Italy (1997), ed. I. Iori, Ricerca scientifica ed educazione permanente, page 396
23. D. Vautherin et al., Phys. Lett. **B191** (1987) 6
24. L. Vinet et al., Nucl. Phys. **A468** (1987) 321